

On the Feasibility of Distributed Phase Synchronization for Coherent Signal Superposition

Alphan Şahin

Department of Electrical Engineering, University South Carolina, Columbia, SC, USA

Email: asahin@mailbox.sc.edu

Abstract—In this study, we analyze the feasibility of distributed phase synchronization for coherent signal superposition, a fundamental enabler for paradigms like coherent over-the-air computation (OAC), distributed beamforming, and interference alignment, under mobility and hardware impairments. With the focus on coherent OAC, we introduce phase-coded pilots (PCPs), a strategy where the radios communicate with each other to eliminate the round-trip phase change in the uplink (UL) and downlink (DL) to align the phase of the received symbol at a desired angle. In this study, considering a carrier frequency offset (CFO)-resilient multi-user procedure, we derive the statistics of the phase deviations to assess how fast the phase coherency degrades. Our results show that residual CFO is a major factor determining the duration of phase coherency, in addition to the non-negligible effects of mobility and the number of nodes in the network. We also provide a proof-of-concept demonstration for coherent signal superposition by using off-the-shelf radios to demonstrate the feasibility of PCPs in practice.

Index Terms—Distributed phase synchronization, phase offset, residual carrier-frequency offset, over-the-air computation.

I. INTRODUCTION

Traditionally, communication and computation are viewed as separate tasks. This approach has been very effective from the engineering perspective, as isolated optimizations can be performed. However, for many computation-oriented applications, the ultimate goal is to compute some mathematical functions (e.g., arithmetic mean, maximum, minimum) of the local information distributed at the different devices rather than the local information itself. In such scenarios, information theoretical results [1] show that harnessing the interference for computation, i.e., *over-the-air computation* (OAC), can provide a significantly higher computation rate than separating communication and computation. The distinct feature of OAC is that it does not acquire the data from each data-generating nodes via typical orthogonal multiple access methods. Instead, all the nodes transmit simultaneously, where the signal superposition in the channel leads to the desired computation result at the receiver; see the surveys in [2]–[4]. Thus, OAC reduces the latency scaled by the number of nodes. Hence, it is a disruptive concept to the traditional way of handling computation and communication independently.

Although promising applications of OAC, such as wireless federated learning (FL) [5], distributed control systems [6], and wireless data centers [7], have been proposed in the

literature, to this date, OAC has not been used in any communication standard or a commercial system. This is partially because realizing a reliable OAC in practice is challenging due to the fading in wireless channels and hardware impairments such as carrier frequency offset (CFO), phase offset (PO), synchronization errors, and imperfect power control. In particular, to achieve *coherent* OAC, the radios must precode their transmissions so that the parameters add up constructively in the complex plane for coherent superposition. Otherwise, the phase of the signals arriving at the receiver will not be the same, destroying the desired coherent aggregation. Thus, the main bottleneck in coherent OAC is to estimate and design the precoder that counteracts the fading channels and hardware impairments, such as CFO and PO [8], [9]. The same issue also arises in several important paradigms, such as interference alignment [10], distributed beamforming [11], [12], and physical-layer network coding [13], as they also rely on phase synchronization. Hence, effective solutions addressing the inevitable imperfections are needed to enable these important paradigms in the next-generation networks.

Given the enabling and fundamental nature of distributed phase synchronization, this paper analyzes its feasibility under hardware impairments and mobility. We introduce *phase-coded pilots* (PCPs), a method that allows the radios to eliminate the round-trip phase change in uplink (UL) and downlink (DL) channels, and discuss a CFO-resilient multi-user procedure based on PCPs for OAC. The proposed approach does not rely on channel reciprocity, and it can be implemented in practice with off-the-shelf software-defined radios (SDRs). In this work, in particular, we derive the statistics of the phase deviations for a given residual CFO and mobility statistics to provide insights into the limits of phase synchronization for OAC, which can also be useful for other paradigms requiring distributed phase synchronization.

Notation: The set of complex numbers is \mathbb{C} . $\mathbb{E}[\cdot]$ is the expectation of its argument. The zero-mean circularly symmetric complex Gaussian distribution with the variance σ^2 , the uniform distribution with the support between a and b , and the Rayleigh distribution with the scale σ are $\mathcal{CN}(\sigma^2, 0)$, $\mathcal{U}_{[a,b]}$, and $\text{Rayleigh}(\sigma)$, respectively. The cumulative distribution function (CDF) of the standard normal distribution is $\Phi(\cdot)$.

II. SYSTEM MODEL

To shed light on how hardware impairment and fading channels affect OAC, consider a scenario with K nodes and

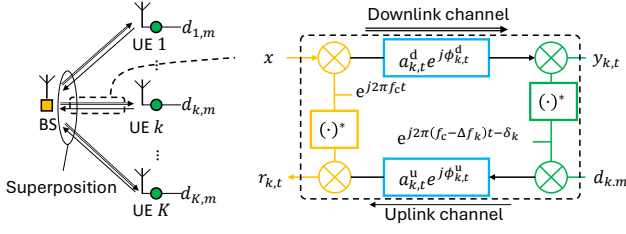


Fig. 1. The channels in UL and DL including environment, CFO, and PO.

one base station (BS), where all the nodes are triggered to transmit simultaneously. Let $d_{k,m} \in \mathbb{C}$ denote the m th parameter at the k th node for $m \in \{0, 1, \dots, M-1\}$ and $k \in \{1, \dots, K\}$, where M is the number of parameters. Suppose that the goal of the BS is to compute $\sum_{k=1}^K d_{k,m}$, $\forall m$, via signal superposition on the complex plane.

Consider the channel model shown in Fig. 1, where $a_{k,t}^u e^{j\phi_{k,t}^u}$ is the UL channel coefficient, $a_{k,t}^d e^{j\phi_{k,t}^d}$ is the DL channel coefficient, and Δf_k and δ_k are the *residual* CFO and the PO with respect to the local oscillator of the BS with the carrier frequency f_c , respectively. We assume that the same oscillator is used at the transmit and receive chains. Without any reciprocity assumption, we model $\phi_{k,t}^d$ and $\phi_{k,t}^u$ as $\phi_{k,0}^d + 2\pi t v_k \cos(\alpha_k)/\lambda$ and $\phi_{k,0}^u + 2\pi t v_k \cos(\alpha_k)/\lambda$, where $\phi_{k,0}^d$ and $\phi_{k,0}^u$ are the random phase shifts in the DL and UL, respectively, $\lambda = c/f_c$ is the wavelength, c is the speed of light, and v_k and α_k denote the velocity for $\alpha_k \sim \mathcal{U}_{[0,2\pi]}$ and the path angle relative to the BS location, respectively.

Suppose that M parameters are transmitted over M orthogonal frequency division multiplexing (OFDM) symbols with the symbol duration T_{ofdm} and the cyclic prefix (CP) duration T_{cp} , where $d_{k,m}$ is mapped to a fixed subcarrier of the m th OFDM symbol, $\forall m$. The received symbol at the BS can be expressed as¹ $s_m = \sum_{k=1}^K r_{k,t}$, where $r_{k,t}$ is the received symbol from the k th node at the BS, and omitting the noise for clarity, it can be expressed as

$$r_{k,t} = a_{k,t}^u e^{j\phi_{k,t}^u} \times e^{-j(2\pi\Delta f_k t + \delta_k)} \times d_{k,m}, \quad t = mT_s, \quad (1)$$

for $T_s \triangleq T_{\text{ofdm}} + T_{\text{cp}}$. Thus, the phase of the received symbol of the k th node is a function of the UL channel, CFO, and PO, and rapidly changes over time as

$$\angle r_{k,t} = \phi_{k,t}^u - 2\pi\Delta f_k t - \delta_k + \angle d_{k,m}. \quad (2)$$

The difficulty for OAC arises from the fact that s_m *cannot* be expressed as $a e^{-j(2\pi\Delta f t + \delta)} \times \sum_{k=1}^K d_{k,m}$, for some parameters a , Δf , and δ , *independent* of the transmitted symbols, in general. Thus, typical estimation and correction methods (e.g., CFO estimation and correction, channel estimation, and linear equalization) relying on the existence of independent parameters like a , Δf , and δ are not helpful in obtaining the desired sum via receiver-only-based processing. Thus, to obtain the desired sum, the transmitters need to precode their

¹The amount of interference due to the *residual* CFO is assumed to be negligible as it is significantly smaller than the subcarrier spacing in practice.

transmission, which fundamentally requires phase synchronization in the network under the hardware imperfections and mobility in the environment.

Let x be a transmitted symbol from the BS in DL. The received symbol at the k th node can be expressed as $y_{k,t} = a_{k,t}^d e^{j\phi_{k,t}^d} \times e^{j(2\pi\Delta f_k t + \delta_k)} \times x$. Hence, the phase of the received symbol at the k th node is also a function of the DL channel, CFO, and PO. Similar to $\angle r_{k,t}$, $\angle y_{k,t}$ also rapidly changes as a function of time as $\angle y_{k,t} = \phi_{k,t}^d + 2\pi\Delta f_k t + \delta_k + \angle x$, where the rotation due to the CFO and PO is in the reverse direction of the one in UL channel (see (2)).

III. PHASE-CODED PILOTS

Suppose that the desired phase is θ_{desired} for the received symbols from *all* nodes at the BS side. To align the phase of the received symbol from the k th node to the desired angle θ_{desired} at the BS side, the BS and the k th node exchange PCPs to estimate and correct the round-trip phase change in the DL and UL. The steps of the proposed procedure, illustrated in Fig. 2, is as follows:

Step 1 (Request): The BS transmits an uncoded pilot symbol p . A pilot is typically a complex number for $|p| = 1$, e.g., a quadrature phase shift keying (QPSK) symbol. Without loss of generality, we assume $p = 1$. The received symbol at the k th node can be expressed as

$$y_{k,t} = a_{k,t}^d e^{j\phi_{k,t}^d} \times e^{j(2\pi\Delta f_k t + \delta_k)} \times p + \omega_k^{(1)}, \quad t = T_k^{(1)},$$

where $\omega_k^{(1)}$ is the noise at the k th node. By using the pilot, the k th node estimates the phase change in the DL as

$$\hat{\theta}_k^{(1)} \triangleq \angle p^* y_{k,t} \big|_{t=T_k^{(1)}} = \phi_{k,T_k^{(1)}}^d + 2\pi\Delta f_k T_k^{(1)} + \delta_k + \psi_k^{(1)},$$

where $\psi_k^{(1)}$ is the phase error due to the noise.

Step 2 (Response): As a response, the k th node transmits a PCP, i.e., $p e^{j\hat{\theta}_k^{(1)}}$, based on the estimated phase change $\hat{\theta}_k^{(1)}$ in Step 1. The received symbol at the BS and the estimated phase change in the UL channel can be written by

$$r_{k,t} = a_{k,t}^u e^{j\phi_{k,t}^u} \times e^{-j(2\pi\Delta f_k t + \delta_k)} \times p e^{j\hat{\theta}_k^{(1)}} + \omega_k^{(2)}, \quad t = T_k^{(2)}$$

and $\hat{\theta}_k^{(2)} \triangleq \angle p^* r_{k,t} \big|_{t=T_k^{(2)}}$ is given by

$$\begin{aligned} \hat{\theta}_k^{(2)} &= \hat{\theta}_k^{(1)} + \phi_{k,T_k^{(2)}}^u - (2\pi\Delta f_k T_k^{(2)} + \delta_k) + \psi_k^{(2)} \\ &= 2\pi\Delta f_k (T_k^{(1)} - T_k^{(2)}) + \phi_{k,T_k^{(1)}}^d + \phi_{k,T_k^{(2)}}^u + \psi_k^{(1)} + \psi_k^{(2)}, \end{aligned} \quad (3)$$

respectively, where $\omega_k^{(2)}$ is the noise and $\psi_k^{(2)}$ is the phase error due to the noise. As can be seen from (3), the PO δ_k is eliminated and the impact of CFO on the phase is reduced as $2\pi\Delta f_k (T_k^{(1)} - T_k^{(2)}) \approx 0$ for $T_k^{(1)} \approx T_k^{(2)}$. The remaining phase in (3) is the round-trip phase change in DL and UL.

Step 3 (Feedback): In this step, the BS provides feedback regarding the round-trip phase change and θ_{desired} by transmitting a PCP as $p e^{j(\theta_{\text{desired}} - \hat{\theta}_k^{(2)})}$. The received symbol at the k th node for $t = T_k^{(3)}$ can be expressed as

$$y_{k,t} = a_{k,t}^d e^{j\phi_{k,t}^d} \times e^{j(2\pi\Delta f_k t + \delta_k)} \times p e^{j(\theta_{\text{desired}} - \hat{\theta}_k^{(2)})} + \omega_k^{(3)},$$

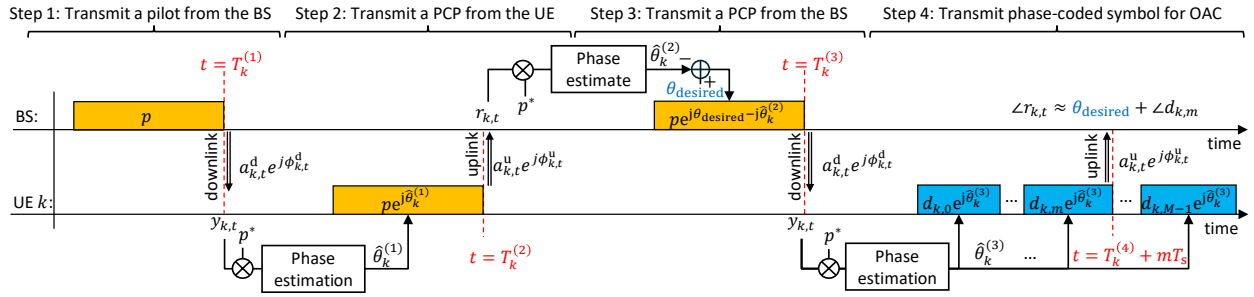


Fig. 2. The basic steps of PCPs to achieve distributed phase synchronization in the network.

where $\omega_k^{(3)}$ is the noise at the k th node. The node then estimates the phase change in the DL channel as

$$\begin{aligned}\hat{\theta}_k^{(3)} &\triangleq \angle p^* y_{k,t} |_{t=T_k^{(3)}} \\ &= \theta_{\text{desired}} - \hat{\theta}_k^{(2)} + \phi_{k,T_k^{(3)}}^d + (2\pi\Delta f_k T_k^{(3)} + \delta_k) + \psi_k^{(3)} \\ &= \theta_{\text{desired}} + 2\pi\Delta f_k (T_k^{(3)} + T_k^{(2)} - T_k^{(1)}) + \delta_k \\ &\quad + \phi_{k,T_k^{(3)}}^d - \phi_{k,T_k^{(1)}}^d - \phi_{k,T_k^{(2)}}^u + \psi_k^{(3)} - \psi_k^{(2)} - \psi_k^{(1)},\end{aligned}$$

where $\psi_k^{(3)}$ is the phase error due to the noise.

Step 4 (Aggregation): Finally, for OAC, the k th node transmits the phase-coded parameter, i.e., $d_{k,m} e^{j\hat{\theta}_k^{(3)}}$, for coherent superposition. The m th received symbol can be written by $s_m = \sum_{k=1}^K r_{k,t} + \omega_m^{(4)}$, $t = T_k^{(4)} + mT_s$, where $\omega_m^{(4)}$ is the noise on the m th superposed symbol s_m and $r_{k,t}$ is given by

$$r_{k,t} = a_{k,t}^u e^{j\phi_{k,t}^u} \times e^{-j(2\pi\Delta f_k t + \delta_k)} \times d_{k,m} e^{j\hat{\theta}_k^{(3)}}. \quad (4)$$

Thus, the angle of $r_{k,t}$ can be expressed as

$$\begin{aligned}\hat{\theta}_{k,m}^{(4)} &\triangleq \angle r_{k,t} |_{t=T_k^{(4)} + mT_s} \\ &= \hat{\theta}_k^{(3)} + \phi_{k,T_k^{(4)} + mT_s}^u - (2\pi\Delta f_k (T_k^{(4)} + mT_s) + \delta_k) \\ &= \theta_{\text{desired}} + \angle d_{k,m} + \theta_{k,m}^{\text{cfo}} + \theta_{k,m}^{\text{mob}} + \theta_{k,m}^{\text{noise}},\end{aligned} \quad (5)$$

for

$$\theta_{k,m}^{\text{cfo}} \triangleq 2\pi\Delta f_k (T_k^{(3)} - T_k^{(4)} + T_k^{(2)} - T_k^{(1)} + mT_s), \quad (6)$$

$$\begin{aligned}\theta_{k,m}^{\text{mob}} &\triangleq \phi_{k,T_k^{(4)} + mT_s}^d - \phi_{k,T_k^{(2)}}^d + \phi_{k,T_k^{(3)}}^u - \phi_{k,T_k^{(1)}}^u \\ &= 2\pi \frac{v_k \cos(\alpha_k) (T_k^{(3)} - T_k^{(1)} + T_k^{(4)} - T_k^{(2)} + mT_s)}{\lambda},\end{aligned} \quad (7)$$

and $\theta_{k,m}^{\text{noise}} \triangleq \psi_k^{(3)} - \psi_k^{(2)} - \psi_k^{(1)}$. Hence, $\angle r_{k,t}$ in the last step is approximately equal to $\theta_{\text{desired}} + \angle d_{k,m}$ for $\theta_{k,m}^{\text{cfo}} + \theta_{k,m}^{\text{mob}} + \theta_{k,m}^{\text{noise}} \approx 0$ radians, where the phase error is a function of the amount of residual CFO, the timing of the exchanged packets, the mobility in the environment, and the noise at the radios.

A. CFO-Resilient Procedure for Multiple Nodes

One of the key observations from (6) is that the impact of the residual CFO of the phase synchronization can be mitigated considerably for $T_k^{(4)} - T_k^{(3)} \approx T_k^{(2)} - T_k^{(1)}$. To exploit this key property, we propose a procedure for multiple

nodes, where the order of the nodes are reversed during the UL and DL transmissions such that $T_k^{(4)} - T_k^{(3)} = T_k^{(2)} - T_k^{(1)}$ holds for *all* nodes. To elaborate the proposed method, let T_p be the packet duration for each aforementioned step.

As shown in Fig. 3, before the OAC phase, a phase-synchronization phase is initiated by the BS by transmitting a request packet including a pilot without any phase coding (i.e., Step 1), common for all K nodes. Once the nodes receive the request packet (i.e., $T_k^{(1)} = 0$), each node access the channel in an order and transmits a response packet in the UL, including a PCP (i.e., Step 2). Let g_u be the minimum response time of a node after it receives a packet. Thus, the instant of the received response packet of the k th node at the BS can be expressed as $T_k^{(2)} = g_u + kT_p$. The BS then transmit feedback packets, including PCPs (i.e., Step 3), for the all nodes in the reverse order. For instance, the first feedback symbol is for the node transmitting the last response packet in the UL. Similarly, the last feedback symbol is for the node transmitting the first response packet, as can be seen in Fig. 3. Let g_d be the response time of the BS. We can then express the instant of the received feedback symbol at the k th node as $T_k^{(3)} = g_u + g_d + (2K + 1 - k)T_p$.

After all the nodes receive the feedback symbols, the nodes transmit the phase-coded OAC symbols, simultaneously, during the OAC phase, and the OAC symbol is received at $T_k^{(4)} = 2g_u + g_d + (2K + 1)T_p$. Thus, the proposed procedure maintains an identical time difference for all nodes, i.e., $T_k^{(2)} - T_k^{(1)} = T_k^{(4)} - T_k^{(3)} = g_u + kT_p$, $\forall k$, eliminating the impact of the residual CFOs of all nodes on the first OAC symbol. With the proposed procedure, (6) can be re-expressed as $\theta_{k,m}^{\text{cfo}} = 2\pi\Delta f_k mT_s$. Now, suppose that $\Delta f_k \sim \mathcal{N}(\sigma_{\text{cfo}}^2, 0)$ holds for all nodes, where σ_{cfo}^2 is the variance of the residual CFO in the network. Hence, $\theta_{k,m}^{\text{cfo}}$ can be modeled as a zero-mean Gaussian random variable with

$$\mathbb{E}[|\theta_{k,m}^{\text{cfo}}|^2] = 4\pi^2 m^2 T_s^2 \sigma_{\text{cfo}}^2. \quad (8)$$

Note that $\theta_{k,m}^{\text{cfo}}$ and $\mathbb{E}[|\theta_{k,m}^{\text{cfo}}|^2]$ do *not* depend on the duration of the phase-synchronization phase with the proposed procedure, therefore, the number of nodes in the network.

1) *The Impact of Noise on Phase Synchronization:* To analyze the impact of the noise on phase synchronization, i.e., $\psi_k^{(1)}$, $\psi_k^{(2)}$, and $\psi_k^{(3)}$, let us consider a generic expression as $r = ae^{j\theta} + \omega$ for $\omega = ne^{j\phi}$. We can then express the angle

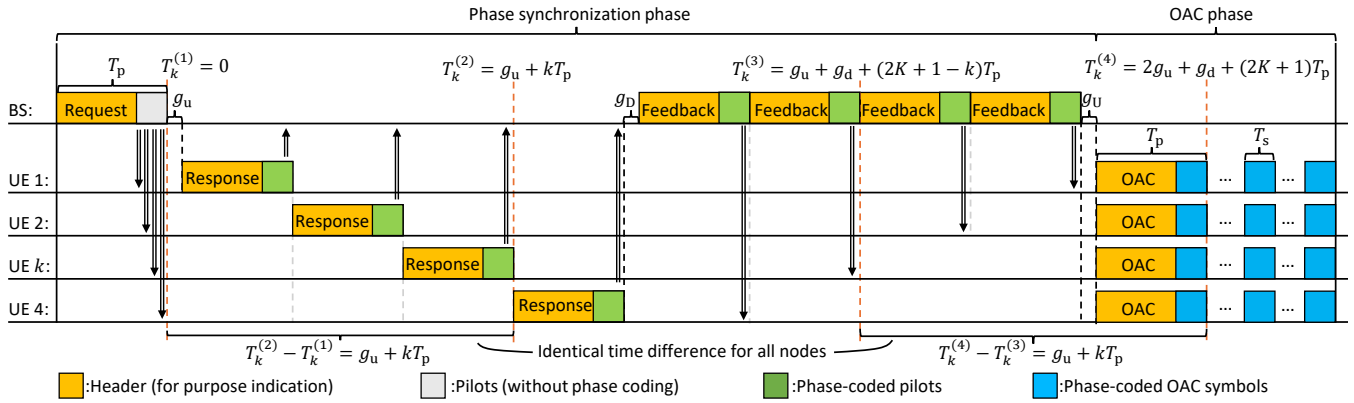


Fig. 3. CFO-resilient multi-user protocol with PCPs. Since $T_k^{(4)} - T_k^{(3)} = T_k^{(2)} - T_k^{(1)}$ holds for *all* nodes, $\theta_{k,m}^{\text{cfo}}$ is not a function of number of nodes.

of r as $\theta + \psi$ for $\psi = \tan^{-1} \left(\frac{n \sin(\phi - \theta)}{a + n \cos(\phi - \theta)} \right) \approx \frac{n}{a} \sin(\phi - \theta)$, where the approximation holds for $n \ll a$. As the argument of the sine function is uniformly distributed, ψ can be modeled as a zero-mean random variable with the variance of $\sigma_n^2 / (2a_k)$ for $\omega \sim \mathcal{CN}(\sigma_n^2, 0)$ and $n \ll a$. Therefore, by assuming independent random variables $\omega_k^{(1)}, \omega_k^{(2)}$, and $\omega_k^{(3)}$ for $\omega_k^{(1)}, \omega_k^{(2)} \sim \mathcal{CN}(\sigma_{\text{noise@BS}}^2, 0)$ and $\omega_k^{(2)} \sim \mathcal{CN}(\sigma_{\text{noise@UE}}^2, 0)$, the phase deviation due to the noise, i.e., $\theta_{k,m}^{\text{noise}}$, can be approximated as a zero-mean Gaussian random variable with

$$\mathbb{E}[|\theta_{k,m}^{\text{noise}}|^2] = \frac{\sigma_{\text{noise@BS}}^2}{2a_{k,T_k^{(2)}}^u} + \frac{\sigma_{\text{noise@UE}}^2}{2a_{k,T_k^{(3)}}^d} + \frac{\sigma_{\text{noise@UE}}^2}{2a_{k,T_k^{(1)}}^d}. \quad (9)$$

2) *The Impact of Mobility on Phase Synchronization:* For the proposed procedure, (7) can be re-expressed as

$$\theta_{k,m}^{\text{mob}} = \frac{2\pi v_k \cos(\alpha_k)}{\lambda} (2(g_u + g_d + (2K + 1 - k)T_p) + mT_s).$$

For the velocity distribution, one may consider two models. For the first model, $v_k = v$ is fixed for all nodes. In this case, $\theta_{k,m}^{\text{mob}}$ is a zero-mean random variable following the Jakes spectrum with

$$\mathbb{E}[|\theta_{k,m}^{\text{mob}}|^2] = \frac{2\pi^2 v^2}{\lambda^2} (2(g_u + g_d + (2K + 1 - k)T_p) + mT_s)^2, \quad (10)$$

For the second model, v_k is a random variable with Rayleigh distribution with the mean \bar{v} , leading to a zero-mean Gaussian $\theta_{k,m}^{\text{mob}}$ with

$$\mathbb{E}[|\theta_{k,m}^{\text{mob}}|^2] = \frac{8\pi \bar{v}^2}{\lambda^2} (2(g_u + g_d + (2K + 1 - k)T_p) + mT_s)^2, \quad (11)$$

The second model's advantage is that the distribution of phase deviations can be analyzed analytically, discussed next.

3) *Phase Deviation Distribution:* Let $\angle d_{k,m}$ be 0. Hence, by using (8), (9), and (10) (or (11)) we can express the root-mean-square error (RMSE) of $\hat{\theta}_{k,m}^{(4)}$ for the k th node as

$$\text{RMSE}_k\{\hat{\theta}_{k,m}^{(4)}\} = \mathbb{E}[|\hat{\theta}_{k,m}^{(4)} - \theta_{\text{desired}}|^2]^{\frac{1}{2}} = \sigma_{k,m}^{\text{err}}. \quad (12)$$

where $\sigma_{k,m}^{\text{err}} \triangleq (\mathbb{E}[|\theta_{k,m}^{\text{noise}}|^2] + \mathbb{E}[|\theta_{k,m}^{\text{mob}}|^2] + \mathbb{E}[|\theta_{k,m}^{\text{cfo}}|^2])^{\frac{1}{2}}$ is the standard deviation of the phase errors for the k th node and m th OAC symbol. Since $\theta_{k,m}^{\text{noise}}, \theta_{k,m}^{\text{cfo}}$, and $\theta_{k,m}^{\text{mob}}$ can be modeled as zero-mean Gaussian random variables with the variances given in (8), (9), and (11), respectively, finally, the CDF of the absolute phase deviations can be calculated as

$$\Pr(|\hat{\theta}_{k,m}^{(4)}| \leq \theta) = 2\Phi\left(\frac{\theta}{\sigma_{k,m}^{\text{err}}}\right) - 1. \quad (13)$$

4) *Computation Rate:* The proposed procedure consumes $2g_u + g_d + 2(K + 1)T_p + (M - 1)T_s$ seconds to compute M functions over a single OFDM subcarrier. Hence, its computation rate is $MT_{\text{ofdm}} / (2g_u + g_d + 2(K + 1)T_p + (M - 1)T_s)$ functions/(s·Hz). Note that the computation rate of the traditional first-communicate-then-compute approach can be approximated as $r_{\text{eff}} / (QK)$ functions/(s·Hz), where r_{eff} is the spectral efficiency in bits/(s·Hz) and Q is the number of bits for parameter quantization.

IV. NUMERICAL RESULTS

In this section, we assess the proposed procedure numerically for $K \in \{5, 10, 20\}$ nodes, $v = \{0.1, 1.5\}$ m/s (for (10)), $\bar{v} = \{0.1, 1.5\}$ m/s (for (11)), $\sigma_{\text{cfo}}^2 \in \{100, 1000\}$, $f_c = 1.8$ GHz, $g_d = g_u = 16$ μ s, $T_{\text{ofdm}} = 1/60$ e3 μ s, and $T_{\text{cp}} = T_{\text{ofdm}}/8$. We assume an implementation of the proposed protocol with $T_p = T_s = 18.75$ μ s. We set $\theta_{\text{desired}} = 0$ radians, $a_{k,t}^d = a_{k,t}^u = 1$, $\text{SNR}_{\text{@UE}} \triangleq 1/\sigma_{\text{noise@UE}}^2 \in \{20, 30\}$ dB and $\text{SNR}_{\text{@BS}} \triangleq 1/\sigma_{\text{noise@BS}}^2 \in \{10, 30\}$ dB, assuming a power-control loop in the network.

In Fig. 4, we first compare the computation rates with the proposed procedure and the traditional first-communicate-then-compute approach for $Q = 8$ bits and $r_{\text{eff}} = 4$ bits/(s·Hz). As can be seen from the figure, the computation rate with OAC is notably larger than the one with the traditional approach, and the efficiency of the proposed procedure improves with the number of OFDM symbols for OAC. We next analyze how many OFDM symbols can be used during the OAC phase under mobility and hardware impairments.

In Fig. 5, we assess how the RMSE gradually changes during the OAC phase under various mobility, signal-to-noise

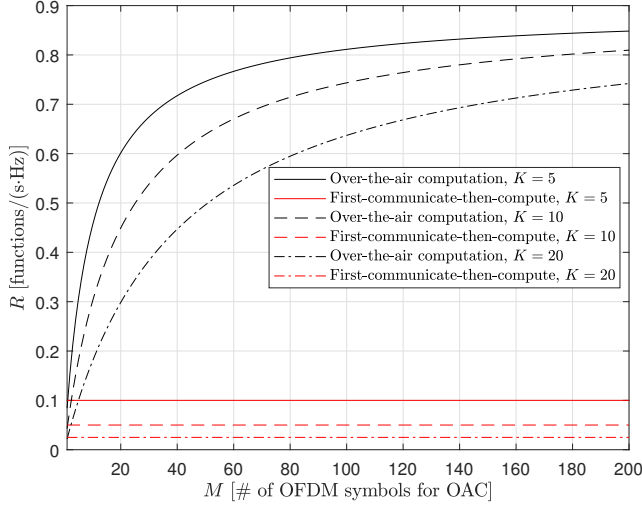


Fig. 4. The computation rate versus the number of OFDM symbols for OAC with the proposed procedure.

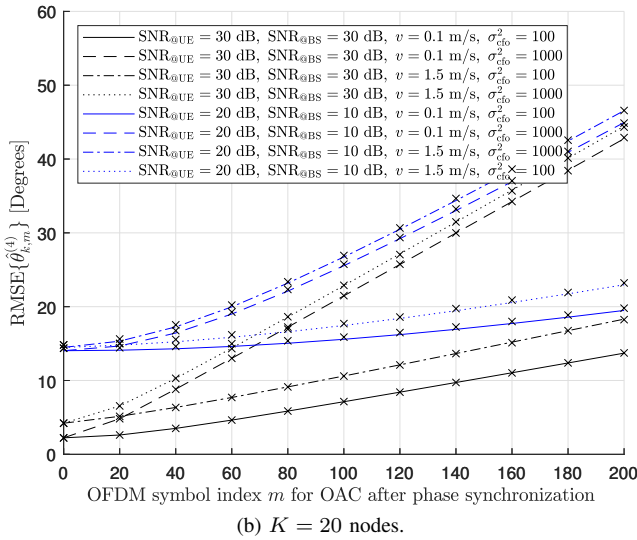
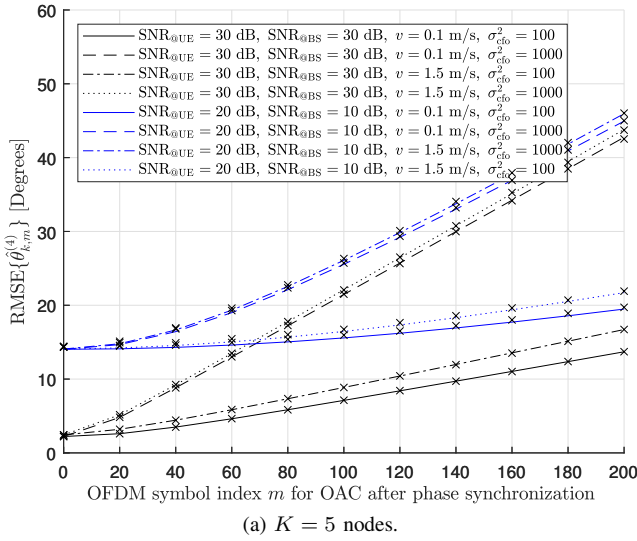
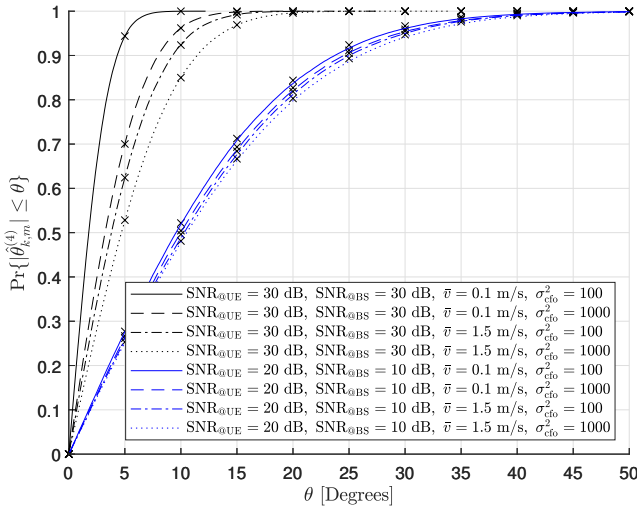


Fig. 5. The RMSE of phase deviations as a function of the OFDM symbol index for the worst node (i.e., $k = 1$) (\times : simulation, lines: theory (12)).

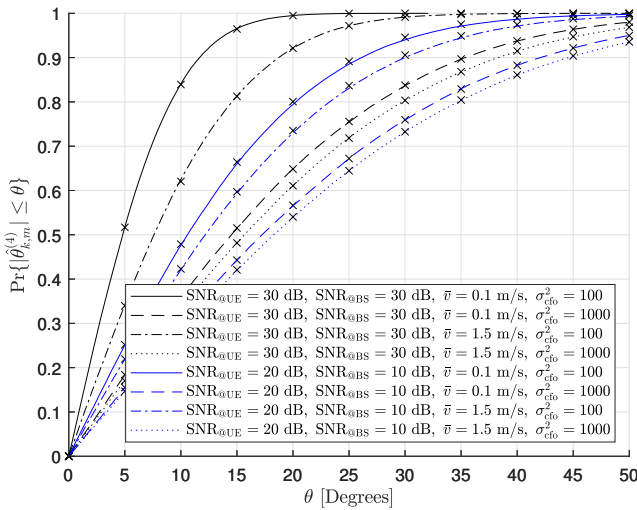
ratio (SNR), and impairment configurations for the worst node, i.e., $k = 1$, for $K \in \{5, 20\}$. Our first observation is that the amount of the noise at the nodes and BS jointly define the minimum RMSE. While the minimum RMSE is about 3° for the high-SNR configurations ($\text{SNR}_{\text{UE}} = \text{SNR}_{\text{BS}} = 30$ dB), it increases to 15° for the low-SNR configurations ($\text{SNR}_{\text{UE}} = 20$ dB, $\text{SNR}_{\text{BS}} = 10$ dB). Secondly, the RMSE gradually increases with m , limiting the number of OFDM symbols in the OAC phase under higher mobility and/or larger CFO variations. For example, assuming that 20° is the maximum tolerable RMSE, $M = 80$ OFDM symbols can be used during the OAC phase for $\sigma_{\text{cfo}}^2 = 1000$, dropping from 200 OFDM symbols for $\sigma_{\text{cfo}}^2 = 100$. Our third observation is that the impact of residual CFO on the phase deviations is more noticeable than the one for the mobility in the channel. For instance, if the mobility increases from 0.1 m/s to 1.5 m/s for $\sigma_{\text{cfo}}^2 = 100$, the RMSE increases slightly. However, if σ_{cfo}^2 is increased from 100 to 1000 for low mobility, the RMSE increases substantially, which indicates the need for an accurate CFO pre-compensation for reliable OAC. Finally, increasing the number of nodes from 5 to 20 has a non-negligible effect on the phase deviations as the duration of the phase synchronization phase increases. Hence, the efficiency of phase synchronization phase needs to be improved to support a large number of nodes. To this end, one effective solution is to parallelize the users within the coherence bandwidth during the phase-synchronization phase. Note that multiple subcarriers within the coherence bandwidth can also be exploited to improve SNR_{UE} and SNR_{BS} .

In Fig. 6, we analyze the distribution of the phase deviations for $m \in \{20, 100\}$ for $K = 20$ nodes. In Fig. 6(a), for all high-SNR configurations, $\Pr(|\hat{\theta}_{k,m}^{(4)}| > 15^\circ)$ is 5%, while it increases to 30% for all low-SNR configurations. In Fig. 6(b), we perform the same analysis for the 100th OFDM symbol. For the scenario with high SNR, large CFO variation, and high mobility, the probability increases to 50% for $m = 100$ th OFDM symbol, indicating a major limitation in the duration of OAC phase. We also observe that residual CFO degrades the phase coherency more quickly than the mobility.

Finally, in Fig. 7, we provide a proof-of-concept demonstration by using Adalm Pluto SDRs. In this demo, the SDRs are triggered to transmit a phase-coded ramp and a sine function simultaneously as test waveforms, respectively, to demonstrate the coherent superposition. To this end, we modify the field-programmable gate array (FPGA) of the SDRs such that the radios estimate the phases in the UL and DL directions. We do not use *any* auxiliary synchronization method (e.g., GPS) for the plausibility of demo. In Fig. 7, we show the IQ data samples at the BS while the BS, UE1, and UE2 transmit. Fig. 7 shows that the phase of each signal is well-aligned at 0° (i.e., the samples at quadrature are almost zero-valued) and the signals coherently superpose, which demonstrates the feasibility of phase synchronization with PCPs. We refer the reader to our 802.11 AI/ML standard contribution in [14] for further details due to the page limitations in this study.



(a) The distribution for the $m = 20$ th OFDM symbol ($K = 20$ nodes).



(b) The distribution for the $m = 100$ th OFDM symbol ($K = 20$ nodes).

Fig. 6. The CDF of the absolute phase deviations (\times : theory (13), lines: simulation). The residual CFO degrades the phase coherency considerably.

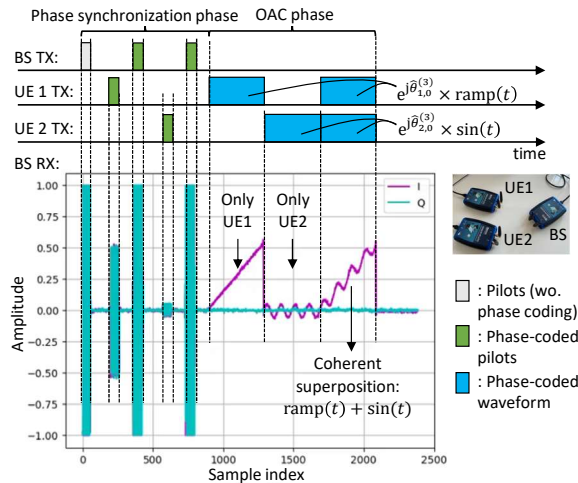


Fig. 7. Proof-of-concept demonstration for coherent signal superposition with PCPs with off-the-shelf SDRs. The BS's signal saturates at its TX and RX antennas are adjacent to each other.

V. CONCLUDING REMARKS

In this study, we analyze the phase synchronization in a network for OAC. With the proposed approach, the nodes and BS exchange PCPs such that the OAC symbols are aligned at a desired phase at the BS during the OAC phase by eliminating the round-trip phase change. We theoretically analyze the phase deviations and derive the RMSE and statistics of the phase deviation as a function of the OFDM symbol index for a given set of parameters such as residual CFO, velocity, the SNR in the UL and DL directions, number of nodes, and packet duration. We also provide proof-of-concept demonstration by using off-the-shelf SDRs to show the feasibility of the PCPs. Our results indicate that residual CFO is a primary limitation for maintaining phase-coherency in the network and gradually destroys the coherency over time more quickly than the mobility in the channel. The extension of this work will provide more details on hardware implementation and analysis regarding amplitude alignment.

ACKNOWLEDGMENT

The author would like to thank Rui Yang and his team at InterDigital for the comprehensive discussions on PCPs.

REFERENCES

- [1] S.-W. Jeon, C.-Y. Wang, and M. Gastpar, "Computation over Gaussian networks with orthogonal components," *IEEE Transactions on Information Theory*, vol. 60, no. 12, pp. 7841–7861, 2014.
- [2] A. Şahin and R. Yang, "A survey on over-the-air computation," *IEEE Commun. Surveys Tuts.*, vol. 25, no. 3, pp. 1877–1908, Apr. 2023.
- [3] Z. Wang, Y. Zhao, Y. Zhou, Y. Shi, C. Jiang, and K. B. Letaief, "Over-the-air computation for 6G: Foundations, technologies, and applications," *IEEE Internet of Things Journal*, pp. 1–25, 2024.
- [4] A. Pérez-Neira, M. Martínez-Gost, A. Şahin, S. Razavikia, C. Fischione, and K. Huang, "Waveforms for computing over the air," 2024. [Online]. Available: <https://arxiv.org/abs/2405.17007>
- [5] X. Cao, Z. Lyu, G. Zhu, J. Xu, L. Xu, and S. Cui, "An overview on over-the-air federated edge learning," *IEEE Wireless Communications*, vol. 31, no. 3, pp. 202–210, 2024.
- [6] S. Cai and V. K. N. Lau, "Modulation-free M2M communications for mission-critical applications," *IEEE Transactions on Signal and Information Processing over Networks*, vol. 4, no. 2, pp. 248–263, 2018.
- [7] X. Wu, S. Zhang, and A. Özgür, "STAC: Simultaneous transmitting and air computing in wireless data center networks," *IEEE J. Sel. Areas Commun.*, vol. 34, no. 12, pp. 4024–4034, 2016.
- [8] H. Guo, Y. Zhu, H. Ma, V. K. N. Lau, K. Huang, X. Li, H. Nong, and M. Zhou, "Over-the-air aggregation for federated learning: Waveform superposition and prototype validation," *Journal of Communications and Information Networks*, vol. 6, no. 4, pp. 429–442, 2021.
- [9] L. You, X. Zhao, R. Cao, Y. Shao, and L. Fu, "Broadband digital over-the-air computation for wireless federated edge learning," *IEEE Trans. Mobile Comput.*, vol. 23, no. 5, pp. 5212–5228, 2024.
- [10] N. N. Moghadam, H. Farhadi, P. Zetterberg, M. N. Khormuji, and M. Skoglund, "Interference alignment — practical challenges and test-bed implementation," in *Contemp. Issues in Wireless Commun.*, 2014.
- [11] R. Mudumbai, G. Barriac, and U. Madhow, "On the feasibility of distributed beamforming in wireless networks," *IEEE Transactions on Wireless Communications*, vol. 6, no. 5, pp. 1754–1763, 2007.
- [12] S. R. Mghabghab and J. A. Nanzer, "Open-loop distributed beamforming using wireless frequency synchronization," *IEEE Transactions on Microwave Theory and Techniques*, vol. 69, no. 1, pp. 896–905, 2021.
- [13] S. Katti, H. Rahul, W. Hu, D. Katabi, M. Medard, and J. Crowcroft, "XORs in the air: Practical wireless network coding," *IEEE/ACM Transactions on Networking*, vol. 16, no. 3, pp. 497–510, 2008.
- [14] A. Şahin et al., "Feasibility study of phase-synchronization for wireless federated learning on WLAN," *IEEE 802.11-25/304r0*, Mar. 2025.